Nickel variability in Hawaiian olivine: Evaluating the relative contributions from mantle and crustal processes

Kendra J. Lynn*, Thomas Shea, and Michael O. Garcia

*kjlynn@hawaii.edu

Department of Geology and Geophysics, University of Hawai‘i, Honolulu, HI 96822, USA

METHODS

XRF Analyses. Some Pu‘u ‘Ō‘ō lavas were re-analyzed to investigate anomalous whole-rock Ni measurements. Major and trace (Y, Sr, Rb, Nb, Zr, Ni, Cr, V, Zn, Ce, Ba, and La) whole-rock analyses were made using X-ray fluorescence (XRF) methods at the University of Massachusetts (see Rhodes and Vollinger 2004). All XRF analyses were completed in the same laboratory using the same calibration procedures. Data are reported in Supplementary Table 1.

Microprobe: Glasses. Kīlauea glass compositions were determined using a 15 kV and 10 nA current with a beam diameter of 10 μm. Peak counting times were 50 s for Si, Fe, and K, 40 s for Ti, Al, Mn, Ca, and P, and 30 s for Na. Na was measured in the first round of elements to minimize loss during analyses. Backgrounds for all analyses were measured on both sides of the peak for half the peak counting times. X-ray intensities were converted to concentrations using standard ZAF corrections (Armstrong 1988). Standards for Kīlauea glass analyses include Basaltic Glass from the Juan de Fuca Ridge (Jarosewich et al. 1980; USNM 111240 VG-2) for Si, Al, Fe, Mg, and Ca, Verma Garnet for Mn, Fluor-Apatite (Jarosewich et al. 1980; USNM 104021) for P, Sphene Glass for Ti, Amelia Albite for Na, and Orthoclase for K. Two sigma relative precision for analyses, based on repeated analysis of Juna de Fuca Ridge glass, are 0.5

wt% for SiO_2, 0.25 wt% for Al_2O_3, 0.2 wt% CaO and FeO, and 0.1 wt% for TiO_2, MnO, MgO, Na_2O, K_2O and P_2O_5. Analyses with totals < 99.0 wt% or > 100.5 wt% were rejected. Kīlauea glass data are an average of 10 to 12 replicate analyses. For analytical conditions and procedures for Koʻolau dike glass, see Haskins and Garcia (2004).

DISCUSSION

Comparison of $Kd^{ol/melt}_{Fe\text{-}Mg}$ to Toplis (2005). Fractional crystallization models of olivine compositions were calculated along a liquid line of descent from each volcano's parental magma composition using the $D^{ol/melt}_{Ni}$ from Matzen et al. (2013), with $D^{ol/melt}_{Mg}$ calculated from Putirka (2008) and a constant $Kd^{ol/melt}_{Fe\text{-}Mg}$ of 0.32 (Putirka et al. 2011). This method was chosen because they recently reviewed the accuracy of previous partitioning approaches (e.g. Hart and Davis 1978, Kinzler et al. 1990, Beattie et al. 1991, Toplis 2005, Li and Ripley 2010, Putirka et al. 2011) when refining their partitioning expression. A comparison of our crystallization models with $D^{ol/melt}_{Ni}$ from Matzen et al. (2013) and the melt concentration dependent $Kd^{ol/melt}_{Fe\text{-}Mg}$ of Toplis (2005) showed no difference in olivine compositions > Fo_{88} (Fig. S1).

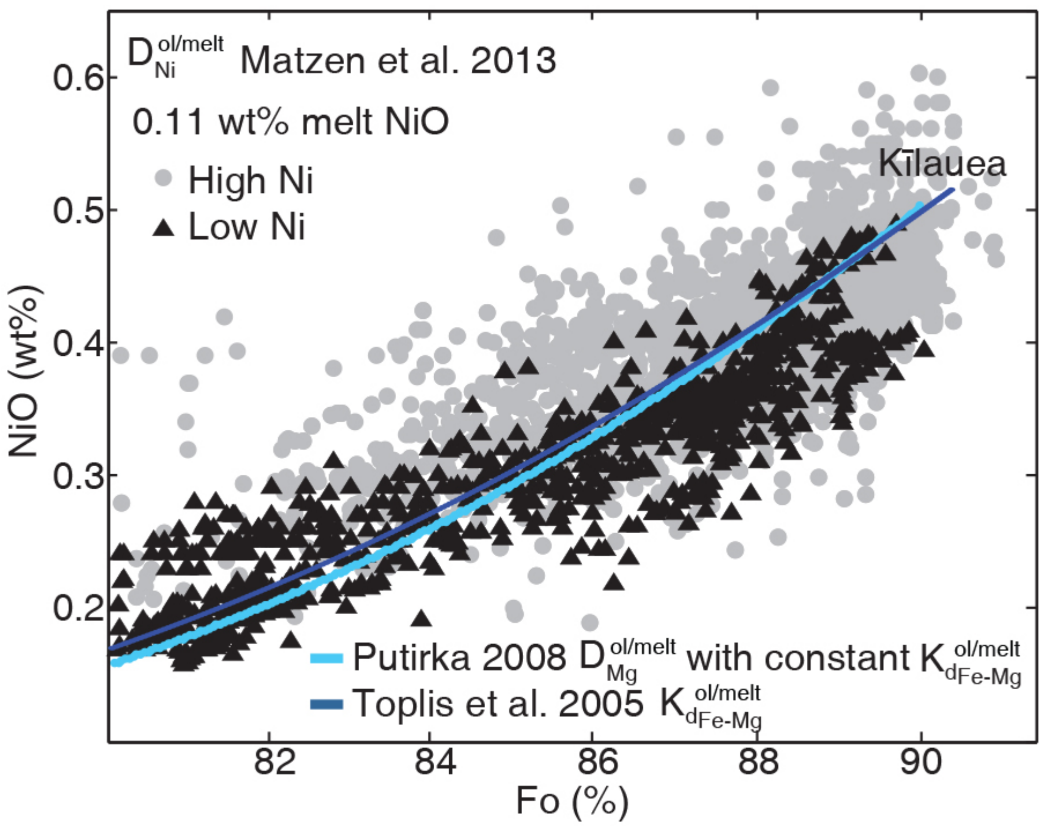

Figure S1: A comparison of fractional crystallization curves along a liquid line of descent for Kīlauea's parental melt composition with 0.11 wt% NiO. At compositions of > Fo_{88}, no differences in Fo-NiO are discernable.

Effect of SiO_2 on Ni diffusivity in olivine. Diffusive re-equilibration of Ni in olivine has been shown to be slower in lower SiO_2 magmas (e.g. Kīlauea) compared to higher SiO_2 magmas (e.g. Ko'olau; Zhukova et al. 2014). To determine whether inter-volcano variations in melt SiO_2 affect the rate of Ni diffusion (and thus different degrees of Fo-NiO decoupling) the activity of silica ($a$$SiO_2$) was determined in Ko'olau and Kīlauea glasses using a supplemental MELTS calculator (Ghiorso and Sack 1995) and used to calculate Ni diffusivities using the methods of Zhukova et al. (2014). The 1-5 wt% difference in SiO_2 between the volcanoes has a negligible effect on Ni diffusivity (see Supplementary Data File 3 for glass analyses and diffusivity calculations). Inter-volcano melt SiO_2 variations are unlikely to influence Fo-NiO decoupling, which is therefore chiefly a signature of magma mixing in crustal environments.

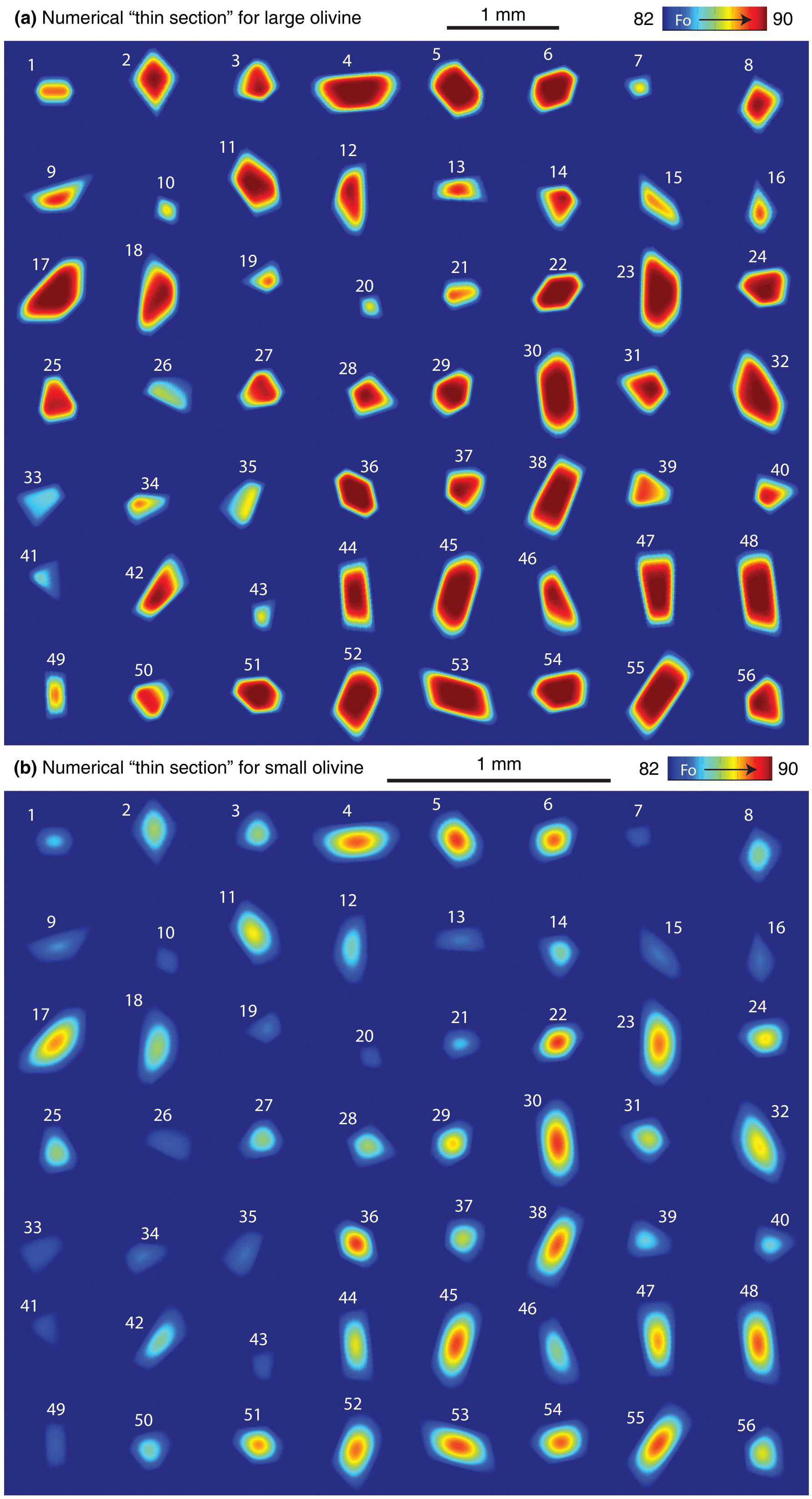

Figure S2. Numerical thin sections for 800 µm (a) and 400 µm (b) crystal sizes (see scale bars). Compositions and model parameters are the same in both, the crystal size is the only difference.

Table S1: Core compositions for the 56 sections in 800 and 400 µm numerical olivine diffusion models presented in Figure S1. Additional data in Supplementary Data File 4.

	800 µm Crystal				400 µm Crystal			
Section[a]	**Fo (%)**	**NiO (wt%)**	**MnO (wt%)**	**Xpx (%)**	**Fo (%)**	**NiO (wt%)**	**MnO (wt%)**	**Xpx (%)**
Initial	**90.0**	**0.600**	**0.130**	**77**	**90.0**	**0.600**	**0.130**	**77**
1	88.1	0.549	0.153	83	84.6	0.404	0.198	83
2	89.9	0.599	0.131	77	86.1	0.487	0.178	87
3	89.5	0.589	0.136	80	85.8	0.464	0.183	86
4	90.0	0.600	0.130	77	88.2	0.564	0.152	84
5	90.0	0.600	0.130	77	88.6	0.573	0.148	83
6	90.0	0.600	0.130	77	88.2	0.562	0.152	84
7	87.2	0.526	0.165	85	83.2	0.338	0.214	78
8	89.8	0.597	0.132	77	85.7	0.467	0.184	87
9	88.9	0.576	0.144	81	84.1	0.393	0.203	83
10	87.2	0.526	0.165	86	83.3	0.339	0.214	78
11	90.0	0.599	0.131	77	86.8	0.514	0.170	87
12	89.6	0.590	0.136	78	85.3	0.451	0.189	86
13	88.9	0.573	0.145	80	84.0	0.386	0.205	83
14	89.3	0.579	0.140	78	85.5	0.455	0.186	86
15	87.7	0.544	0.158	86	83.9	0.375	0.206	81
16	88.5	0.565	0.149	83	83.9	0.374	0.207	81
17	90.0	0.600	0.130	77	87.8	0.549	0.158	85
18	89.8	0.596	0.132	77	86.1	0.483	0.179	87
19	87.9	0.544	0.156	84	83.9	0.373	0.206	81
20	86.7	0.501	0.173	84	83.1	0.329	0.216	76
21	88.0	0.544	0.155	83	84.5	0.399	0.199	82
22	90.0	0.600	0.130	77	88.6	0.574	0.148	83
23	90.0	0.600	0.130	77	88.1	0.559	0.154	85
24	89.9	0.599	0.131	77	87.2	0.525	0.165	86
25	89.3	0.584	0.138	80	86.0	0.473	0.180	86
26	85.2	0.438	0.190	85	83.3	0.335	0.213	76
27	89.5	0.590	0.136	79	85.9	0.470	0.181	86
28	89.9	0.598	0.132	77	86.1	0.485	0.178	87
29	90.0	0.599	0.131	77	87.3	0.531	0.163	86
30	90.0	0.600	0.130	77	88.6	0.574	0.147	83
31	89.9	0.598	0.131	77	86.5	0.502	0.173	87
32	90.0	0.599	0.131	77	87.2	0.528	0.165	86
33	85.0	0.412	0.195	80	83.1	0.318	0.217	74
34	87.4	0.523	0.163	84	83.8	0.370	0.207	81
35	86.2	0.467	0.172	89	83.8	0.361	0.208	79
36	90.0	0.600	0.130	77	88.6	0.574	0.148	83
37	89.7	0.595	0.134	78	86.2	0.486	0.177	86
38	90.0	0.600	0.130	77	88.3	0.566	0.151	84
39	88.3	0.550	0.152	82	85.0	0.425	0.193	84
40	89.2	0.576	0.142	77	85.0	0.433	0.192	85

41	84.4	0.381	0.201	80	83.0	0.312	0.218	74
42	89.9	0.598	0.132	77	85.7	0.469	0.184	87
43	86.7	0.506	0.171	86	83.2	0.332	0.215	77
44	90.0	0.600	0.130	77	86.8	0.517	0.170	87
45	90.0	0.600	0.130	77	88.5	0.571	0.150	83
46	89.7	0.593	0.134	78	85.8	0.475	0.182	87
47	90.0	0.600	0.130	77	87.8	0.549	0.158	85
48	90.0	0.600	0.130	77	88.3	0.565	0.152	84
49	88.0	0.549	0.155	84	83.4	0.355	0.212	80
50	88.9	0.572	0.144	81	85.5	0.450	0.187	85
51	90.0	0.600	0.130	77	87.8	0.549	0.157	85
52	90.0	0.600	0.130	77	88.1	0.557	0.154	85
53	90.0	0.600	0.130	77	88.5	0.571	0.149	83
54	90.0	0.600	0.130	77	88.2	0.563	0.152	84
55	90.0	0.600	0.130	77	88.4	0.569	0.150	84
56	89.8	0.595	0.133	78	86.6	0.504	0.172	86

Note(s): [a] Section numbers are assigned on Figure S2

References

Armstrong, J. T. (1988) Quantitative analyses of silicate and oxide materials: Comparison of Monte Carlo, ZAF, and φ(ρz) procedures. In Microbeam Analyses, D.E. Newbury, Ed., San Francisco Press, San Francisco, pp 239-246.

Beattie, P., Ford, C., and Russel, D. (1991) Partition coefficients for olivine-melt and orthopyroxene-melt systems. Contributions to Mineralogy and Petrology, 109, 212-224.

Hart, S.R., and Davis, K.E. (1978) Nickel partitioning between olivine and silicate melt. Earth and Planetary Science Letters, 40, 203-219.

Haskins, E.H., and Garcia, M.O. (2004) Scientific drilling reveals geochemical heterogeneity within the Ko‘olau shield, Hawai‘i. Contributions to Mineralogy and Petrology, 147, 162-188.

Jarosewich, E., Nelen, J.A., and Norberg, J.A. (1980) Reference samples for electron microprobe analysis. Geostandards Newsletters, 4, 43-47.

Kinzler, R.J., Grove, T.L., and Recca, S.J. (1990) An experimental study on the effect of temperature and melt composition on the partition of nickel between olivine and silicate melt. Geochimica et Cosmochimica Acta, 54, 1255-1265.

Li, C., and Ripley, E.M. (2010) The relative effects of composition and temperature on olivine-liquid Ni partitioning: Statistical deconvolution and implications for petrological modeling. Chemical Geology, 275, 99-104.

Putirka, K.D. (2008) Thermometers and barometers for volcanic systems. Reviews in Mineralogy and Geochemistry, 69, 61-120.

Putirka, K., Ryerson, F.J., Perfit, J., and Ridley, W.I. (2011) Mineralogy and composition of the oceanic mantle. Journal of Petrology, 52, 279-313.

Rhodes, J.M., and Vollinger, M.J. (2004) Composition of basaltic lavas sampled by phase-2 of the Hawaii Scientific Drilling Project: Geochemical stratigraphy and magma types. Geochemistry Geophysics Geosystems, 5, doi: 10.1029/2002GC000434.

Toplis, M.J. (2005) The thermodynamics of iron and magnesium partitioning between olivine and liquid: criteria for assessing and predicting equilibrium with natural and experimental systems. Contributions to Mineralogy and Petrology, 149. 22-29.